2 Ice Deformation

2.1 CREEP OF GLACIER ICE

Many laboratory experiments have been conducted to study the creep (or deformation) of ice. These include measurements on the creep of single ice crystals by Glen and Perutz (1954), Steinemann (1954), Rigsby (1958), Readey and Kingery (1964), and Montagnat and Duval (2004); papers discussing the deformation of polycrystalline ice include Glen (1952), Steinemann (1958), Jonas and Müller (1969), Duval (1981), Mellor and Cole (1982), and Jacka and Maccagnan (1984). Extensive reviews on this subject can be found in Weertman (1973a), Hobbs (1974), Glen (1975), Hooke (1981), Budd and Jacka (1989), and Schulson and Duval (2009). Below, a short summary of the most important results is given. For most applications discussed in this book, this elementary review is sufficient; those readers who are interested in a more comprehensive discussion are referred to the in-depth treatment of this topic by Schulson and Duval (2009).

The most common form of ice is Ice Ih with a crystal structure as shown in Figure 2.1. Each molecule consists of an oxygen atom strongly bonded to two hydrogen atoms forming a V shape. These bonds between oxygen and hydrogen atoms are called *covalent bonds*. The resulting H_2O molecule has a slightly positive charge on the side of the two hydrogen atoms and a slightly negative charge on the side of the oxygen atom. As a result, the partially positive hydrogen atom on one water molecule is electrostatically attracted to the partially negative oxygen of a neighboring molecule, forming a weak hydrogen bond (Figure 2.1a). In an ice crystal, each oxygen atom is surrounded by four nearest neighbors arranged near the vertices of a regular tetrahedron centered around the molecule under consideration (Pounder, 1965; Schulson, 1999). Referring to Figure 2.1b, three of the atoms surrounding the central oxygen atom **O** form an equilateral triangle in a plane called the basal plane; these atoms are marked as $\mathbf{O^2}$. The fourth oxygen atom, $\mathbf{O^1}$ is positioned such that the line $\mathbf{O^1O}$ is perpendicular to the basal plane. This direction is referred to as the c-axis (Pounder, 1965).

Next consider the four oxygen atoms surrounding atom $\mathbf{O^1}$. One of these four neighboring atoms is atom **O**, while the other three atoms, marked $\mathbf{O^3}$ also lie in a plane perpendicular to $\mathbf{O^1O}$, forming an inverted tetrahedron centered on $\mathbf{O^1}$. Figure 2.1b shows only how **O** and $\mathbf{O^1}$ are surrounded by four oxygen atoms. The other oxygen atoms, $\mathbf{O^2}$ and $\mathbf{O^3}$, are of course also surrounded by four oxygen atoms but extending the illustration to depict the full three-dimensional structure would make the figure too confusing. Following Pounder (1965), consider therefore the two projections shown in Figure 2.1c and d.

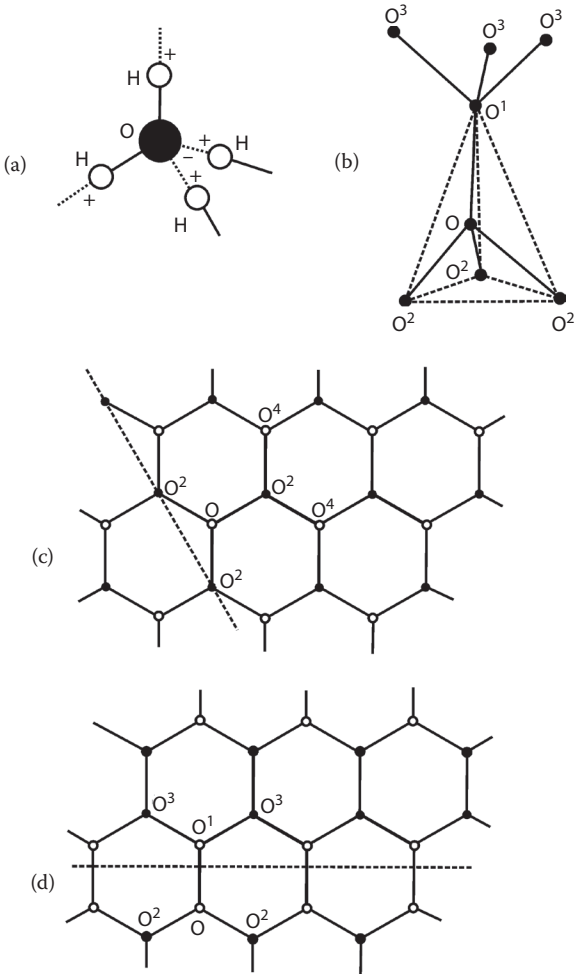

FIGURE 2.1 Crystal structure of ice. (a) placement of oxygen and hydrogen atoms; solid lines represent covalent bonds and dashed lines represent weaker hydrogen bonds. (b) structure of an ice lattice showing the tetrahedral bond arrangement; solid lines represent hydrogen bonds, and dashed lines outline the tetrahedron. (c) projection of the ice lattice on a basal plane; open and filled circles represent oxygen atoms on different planes, and the dashed line gives the direction of the c-axis. (d) projection of the ice lattice on a plane through the c-axis (the plane perpendicular to the dashed line in panel d); the dashed line represents the glide plane. (Panels b–d modified from Pounder, E. R., *Physics of Ice*, Pergamon Press, London, 1965.)

Figure 2.1c shows the arrangement of oxygen atoms projected on the basal plane. Two sets of atoms are shown and distinguished by open and filled circles. The filled circles correspond to atoms lying in the basal plane passing through the three $\mathbf{O^2}$ atoms. The open circles correspond to the next basal plane containing atom **O**. Note that this figure shows only the slanting bonds of the $\mathbf{O^2O}$ type and not the bonds in the direction of the c-axis ($\mathbf{O^1O}$). Atom **O** has three downward slanting bonds to the

three atoms **O²**. Each of these atoms must have three upward slanting bonds, one of which is to atom **O**. The other two slanting bonds are to two atoms, marked **O⁴**, that must lie in the same basal plane as atom **O**. What emerges is a pattern of hexagons that zigzag back and forth between two basal planes (Pounder, 1965).

Now consider the arrangement of oxygen atoms projected on a plane parallel to the c-axis and passing through a pair of **O²** atoms (Figure 2.1d). In this case, open and filled circles represent atoms that are in different vertical planes (with vertical being the direction of the c-axis). The upward bond from atom **O** must be vertical so that the positions of the atoms **O¹** are fixed. Further, each **O³** atom is directly above an **O²** atom. The other allowed geometry would be if the **O³** atoms occupied the vacant centers of the hexagons shown in Figure 2.1d; this is the arrangement found in, for example, diamond (Pounder, 1965). The important consequence of this arrangement is that ice has only one important axis of symmetry, namely, the c-axis; and properties of a single ice crystal may be assumed isotropic in all directions perpendicular to the c-axis, but anisotropy can be expected between properties measured parallel and perpendicular to the c-axis (Pounder, 1965).

To recapitulate, the ice crystal structure is such that oxygen atoms are arranged in approximately parallel planes, called the basal planes. The direction perpendicular to the basal planes is referred to as the c-axis. Deformation of a single crystal occurs readily if there is a component of shear stress acting on the basal plane. In that case, the layers of molecules glide over one another, similar to a deck of cards. Nonbasal glide is much more difficult to initiate and requires much larger stress; for that reason, nonbasal glide is also referred to as hard glide. For the majority of crystal orientations, there will be a component of shear stress in the basal plane; thus it seems reasonable to presume that deformation of ice is achieved mainly by basal glide. An example in which basal glide cannot occur is when a compressive or tensile stress is applied perpendicular to the basal plane. For practical purposes, a crystal in this situation can be considered nondeforming.

Hobbs (1974) argues that polycrystalline ice can deform into any arbitrary shape without changing its volume only if there are at least five independent slip directions. In the basal plane, there are only two (perpendicular) slip directions, and therefore Hobbs (1974) concludes that deformation of polycrystalline ice is probably controlled by nonbasal glide. As noted above, this hard glide is much more difficult to induce than basal glide, so that, under similar conditions, a sample of ice may be expected to deform at a slower rate than a single crystal deforming by basal slip. Experiments suggest that this is indeed the case (c.f. Hobbs, 1974), but there may be an alternative explanation.

The argument that there must be at least five independent slip directions is credited to Taylor (1938), who assumed that deformation occurs uniformly throughout a polycrystalline sample. In that case, the strain in each crystal or volume element must be the same as the bulk deformation of the sample. Because the sample is able to deform in any direction, Taylor's assumption of homogeneous strain implies that each individual crystal must be able to deform into any shape. As shown by Von Mises (1928), this requires at least five independent slip directions (c.f. Hutchinson, 1976). Hutchinson (1977) showed that relaxing the assumption of uniform strain and adopting a self-consistent method reduces the number of required slip directions to four and deformation can be accommodated by basal slip plus slip of basal

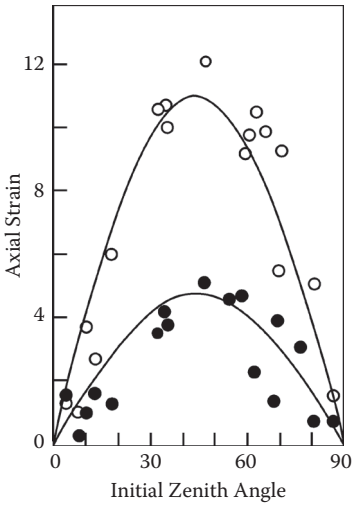

FIGURE 2.2 Axial strain of individual crystals as a function of their initial zenith angle (the angle between the crystal c-axis and the direction of compression) after 3% bulk strain (dots) and after 7% bulk strain (open circles). The two curves represent the theoretical distribution $\varepsilon_c = \pi \varepsilon_b \cos \sin \phi$, with ε_c the crystal strain, ε_b the bulk strain of the aggregate, and ϕ the initial zenith angle of the crystal. (From Azuma, N., and A. Higashi, *Ann. Glaciol.,* 6, 130–134, 1985. Reprinted from the *Annals of Glaciology* with permission of the International Glaciological Society and the authors.)

dislocations on prismatic planes (parallel to the c-axis). The latter slip mode requires larger stresses than basal slip. An alternative possibility is that deformation of a polycrystalline aggregate is achieved by straining only those crystals that are aligned favorably, that is, crystals with a component of shear stress in the basal plane. In a sample of randomly oriented crystals, this is always possible. Because unfavorably oriented crystals deform much more slowly than those that are oriented optimally, the rate of deformation of the sample (which is simply the average of the deformation rates of all crystals in the sample) may be expected to be (much) smaller than the rate of deformation of a single crystal that is favorably aligned. The difficulty with this model is that it is not entirely clear how individual crystals can be strained at different rates without creating voids or overlaps in the aggregate.

Experimental evidence supports the hypothesis that basal glide is the dominant mechanism by which deformation occurs. Azuma and Higashi (1985) subjected a sample with an initially random fabric to compression and measured the uniaxial strain of individual crystals as a function of the initial angle between the compressive axis and the crystal c-axis. The results, shown in Figure 2.2, show that crystals with their c-axis along the compressive axis, or perpendicular to it, undergo very little deformation. This is because these crystals have little or no component of shear stress in their basal plane, and for single crystals, the rate of deformation is proportional to this shear stress. The resolved basal shear stress is largest if the angle between c-axis and direction of compression is 45° and these crystals

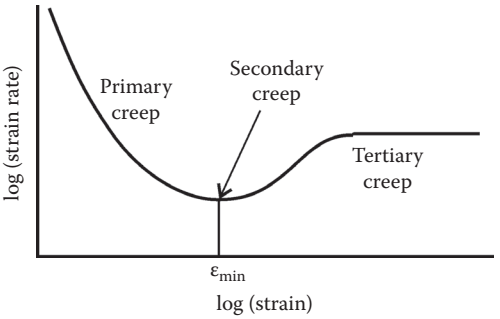

FIGURE 2.3 Typical creep curve for glacier ice as measured in laboratory experiments.

undergo maximum deformation, as indicated by the experiments of Azuma and Higashi (1985).

For single ice crystals subjected to a constant stress and oriented for basal glide, the strain rate initially increases with time until a steady state is reached. Weertman (1973a) argues that the accelerating creep can be attributed to the initially low density of dislocations. Dislocations are line defects bounding areas in a crystal where slip has already taken place. Outward propagation of these dislocations increases the area where slip occurs, resulting in deformation by basal slip (Poirier, 1985). As creep continues, more dislocations are produced by multiplication processes, allowing the creep rate to accelerate. In single ice crystals, this effect appears to be more important than the interaction of dislocations, which causes a decrease in creep rate as observed in metal single crystals.

For a specimen of polycrystalline ice, on the other hand, the rate of deformation decreases rapidly with time after a (constant) stress is applied; this stage is called primary or transient creep (Figure 2.3). The mechanism responsible for the decrease in creep rate remains unknown (Weertman, 1973a; Schulson and Duval, 2009), although it is often suggested that the decrease in creep rate is caused by the formation of dislocation tangles, which inhibit dislocation glide. An alternative explanation is proposed by Van der Veen and Whillans (1994), who argue that the bulk strain rate of a specimen decreases as the sample deforms as a result of progressive rotation of crystal c-axes toward orientations unfavorable for further deformation by basal glide (c.f. Section 2.4).

According to the conventional view, the period of primary creep is followed by a period of secondary creep, during which the strain rate remains approximately constant as deformation continues. Paterson (1994) argues that during secondary creep, the ice may be recrystallizing at grain boundaries where (elastic) stresses are particularly high. The observed constant strain rate probably results from a temporary balance between softening at these boundaries and hardening elsewhere. A different view is expressed by Budd and Jacka (1989), who note that the concept of steady-state secondary creep for ice is invalid because of its inherently transitory nature. The model simulations of Van der Veen and Whillans (1994) support this view and suggest that the minimum creep rate reached during deformation simply marks the onset of recrystallization, which softens the ice by aligning crystals in favorable orientations (c.f. Section 2.4).

After passing through the minimum, the strain rate increases again to, perhaps, a constant value, during what is referred to as tertiary creep. This increase is attributed to recrystallization (Hooke, 1981; Li et al., 1996) and may occur in discrete steps, as suggested by Hooke and Hudleston (1980).

A typical creep curve obtained in the laboratory is shown in Figure 2.3. The common view for modeling glacier flow is that secondary and tertiary creep are most important. Primary creep, if related to long-range interactions between dislocations (Schulson and Duval, 2009), does not occur within the main body of a glacier because this ice has been deforming under a given stress regime for a sufficiently long time to reach the stage of secondary or tertiary creep. Schulson and Duval (2009) suggest that tertiary creep can be described by a similar relation as that used for secondary creep, but with enhancement factors ranging from about 3 in compression or pure shear to between 8 and 10 for simple shear. Secondary creep of anisotropic ice is described by Glen's flow law discussed in Section 2.2. Note that this interpretation is contradictory to the view that primary creep reflects hardening of ice as crystals are oriented and a distinct fabric develops (Van der Veen and Whillans, 1994).

2.2 CONSTITUTIVE RELATION

To arrive at the constitutive relation most often used in glaciology, the analysis of Nye (1953) is followed; a mathematically more rigorous approach can be found in Hutter (1983). The first assumption is that ice is incompressible and that it remains isotropic throughout the flow, with crystal c-axes randomly oriented. In that case, the principal axes of the strain-rate tensor must be parallel to those of the stress tensor. The second assumption is that ice deformation is independent of hydrostatic pressure, and the components of strain rate are proportional to the components of deviatoric stress (Section 1.2). That is,

$$\dot{\varepsilon}_{ij} = \chi \tau_{ij}, \tag{2.1}$$

where χ is a positive scalar function that may depend on the entire stress state, temperature of the ice, and perhaps other factors as well.

The next step is to determine the form of the function χ. Because the constitutive response of glacier ice must be independent of the particular coordinate system chosen, χ must be a function of the invariants of the strain rate and stress deviator tensors. Invariants of a tensor are scalar quantities whose values are not affected by a transformation of the coordinate system (Section 1.1). Both the stress and strain-rate tensors are of second order and therefore have three invariants each. For the deviatoric stress tensor, the invariants are (equations (1.21)–(1.23))

$$I_1 = \tau_{xx} + \tau_{yy} + \tau_{zz}, \tag{2.2}$$

$$I_2 = \tau_{xx}^2 + \tau_{yy}^2 + \tau_{zz}^2 + 2\left(\tau_{xy}^2 + \tau_{xz}^2 + \tau_{yz}^2\right), \tag{2.3}$$

$$I_3 = \det(\tau_{ij}). \tag{2.4}$$

From the definition of deviatoric stresses (equation (1.36)), it follows immediately that the first invariant is zero. By adopting equation (2.1), it also follows that the first invariant of the strain-rate tensor is zero (which is true for any incompressible material). It is now postulated that the rheology of glacier ice is independent of the third invariants of the strain-rate and deviatoric stress tensor. Thus

$$\chi = \chi[I_2(\tau), I_2(\dot{\varepsilon})]. \tag{2.5}$$

Rather than using the second invariants, the quantities called effective strain rate, $\dot{\varepsilon}_e$, and effective stress, τ_e, are used. These are defined through

$$2\dot{\varepsilon}_e^2 = \dot{\varepsilon}_{xx}^2 + \dot{\varepsilon}_{yy}^2 + \dot{\varepsilon}_{zz}^2 + 2\left(\dot{\varepsilon}_{xy}^2 + \dot{\varepsilon}_{xz}^2 + \dot{\varepsilon}_{yz}^2\right), \tag{2.6}$$

$$2\tau_e^2 = \tau_{xx}^2 + \tau_{yy}^2 + \tau_{zz}^2 + 2\left(\tau_{xy}^2 + \tau_{xz}^2 + \tau_{yz}^2\right). \tag{2.7}$$

Based on the laboratory experiments of Glen (1952), Nye (1953) suggested the following relation between the effective stress and effective strain rate

$$\dot{\varepsilon}_e = A\tau_e^n, \tag{2.8}$$

where A and n are the flow parameters. From (2.1) and the definitions of effective stress and strain rate, it follows that

$$\chi = A\tau_e^{n-1}, \tag{2.9}$$

and hence

$$\dot{\varepsilon}_{ij} = A\tau_e^{n-1}\tau_{ij}. \tag{2.10}$$

Equation (2.10) is called Nye's generalization of Glen's law, or Glen's law for short. Virtually all modeling of the flow of glaciers is based on this constitutive relation.

For some applications, the inverse formulation of equation (2.10) is needed, for example when estimating stresses from measured strain rates. Combining (2.10) and (2.8) gives

$$\dot{\varepsilon}_{ij} = A\left(\frac{\dot{\varepsilon}_e}{A}\right)^{1-1/n}\tau_{ij}, \tag{2.11}$$

and

$$\tau_{ij} = B\dot{\varepsilon}_e^{1/n-1}\dot{\varepsilon}_{ij}, \tag{2.12}$$

with

$$B = A^{-1/n}. \tag{2.13}$$

The flow parameters, A and B, are dependent on many factors, most notably the temperature of the ice.

The above derivation is based solely on mathematical considerations of permissible relations between the stress and strain-rate tensors and does not consider the physical processes by which ice deforms. Deformation of crystals results from defects existing in the crystal lattice where the periodicity in which atoms are arranged is locally interrupted. As these defects move around under an applied stress, some deformation of the crystal takes place. Thus, if this deformation can be estimated, and if the concentration of defects and their migration velocity are known, the flow law can be derived on theoretical grounds, at least in principle (Poirier, 1985). While glide of dislocation (line defects) is the primary agent of deformation of polycrystalline ice, other microscopic processes may contribute to observed macroscopic deformation. For example, material may be transported by diffusion (diffusion creep) or by shear along grain boundaries (grain boundary sliding). These two processes are strongly coupled and mutually accommodating. Grain boundary sliding creates voids or overlaps that are accommodated by diffusion creep, and vice versa (Poirier, 1985). Which microscopic process is most important to bulk deformation depends on a number of factors including ice temperature and magnitude of the applied stress. The impossibility of observing microscopic processes in situ on glaciers makes it near impossible to evaluate which process is most important or relevant to glacier flow and under what conditions. For this reason, there is no generally accepted flow law for glacier ice derived from consideration of crystal-scale processes (c.f. Schulson and Duval, 2009). Some alternatives to Glen's law have been proposed, and these are discussed in the next section.

The constitutive relation (2.10), or the inverse formulation (2.12), contains two parameters, namely, the factor n in the exponent and the rate factor A or viscosity parameter B (the latter two are related through equation (2.13)). Many laboratory and field measurements have been conducted to determine the values of these parameters. It should be kept in mind, however, that none of these experiments has unambiguously confirmed the validity of the general form of the constitutive relation, although Schulson and Duval (2009) note that equation (2.11) was verified with tests performed in shear and compression. To determine the form of the constitutive relation, combined shear and compression experiments are needed (Morland, 1979), but most laboratory experiments are uniaxial stress experiments. Interpretation of field data has not led to an unequivocal constitutive relation, either. The major problem is that field measurements yield only strain rates, and to find the relation between strain rate and stress, the stresses must be inferred indirectly. In most cases, the stresses are calculated from a simplified theory, which may greatly affect the resulting correlation. Van der Veen and Whillans (1990) used a full-stress model to simulate flow along the Dye-3, Greenland, strain network and compared field data with model predictions. Adopting various forms of the flow law, their results failed to convincingly verify the applicability of Glen's flow law.

Laboratory experiments generally support values of n around 3 for effective stresses in the range of 200 to 2000 kPa (Hooke, 1981; Budd and Jacka, 1989), in agreement with theoretical considerations (Weertman, 1973a). At stresses more common in glaciers (<200 kPa), the exponent may be less than 3 (including n = 1, describing a Newtonian viscous fluid), but these experiments must be interpreted

with caution because of the great difficulty in conducting such tests and because in many of the experiments, the ice is deformed for only a limited time to strains of a few percent (Weertman, 1973a; Budd and Jacka, 1989; Schulson and Duval, 2009). Nevertheless, analysis of field data and laboratory experiments supports a transition from deformation with $n \approx 3$ at high stresses and $n \leq 2$ at low stresses (Montagnat and Duval, 2004). This issue is discussed further in Section 2.4.

The rate factor determined from laboratory and field experiments applies to (steady-state) secondary creep, linking the minimum strain rate (Figure 2.3) to deviatoric stress. It is widely accepted that the rate factor is an exponential function of temperature. Hooke (1981) evaluated available data and found the following best fit

$$A = A_o \exp\left(-\frac{Q}{RT} + \frac{3C}{(T_r - T)^k} \right), \tag{2.14}$$

or

$$B = B_o \exp\left(\frac{T_o}{T} - \frac{C}{(T_r - T)^k} \right), \tag{2.15}$$

where $A_o = 9.302 \cdot 10^7\ \mathrm{kPa^{-3}\,yr^{-1}}$, $Q = 78.8$ kJ/mol (the activation energy for creep), $R = 8.321$ J/(mol K) (the gas constant), $C = 0.16612\ \mathrm{K^k}$, $T_r = 273.39$ K, $k = 1.17$, $B_o = 2.207 \cdot 10^{-3}\ \mathrm{kPa \cdot yr^{1/3}}$, $T_o = 3155$ K, and the ice temperature, T, is expressed in K (Kelvin). In Figure 2.4 these two relations are shown (dashed lines). Also shown

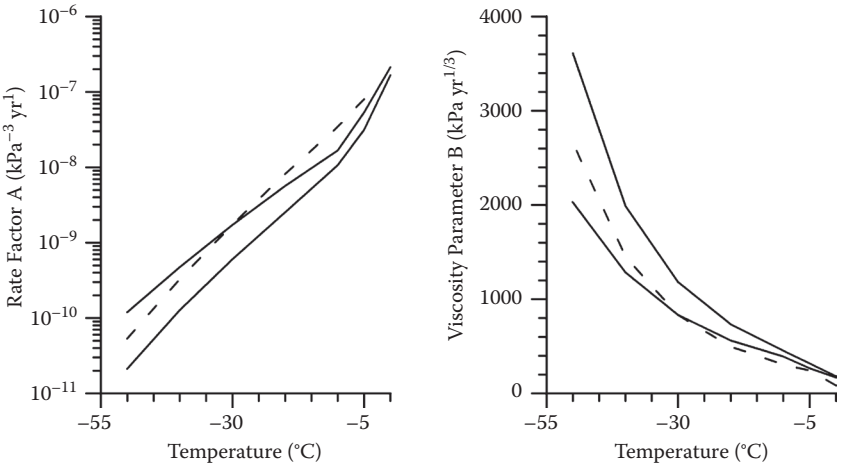

FIGURE 2.4 Rate factor, A, and viscosity parameter, B, as a function of ice temperature. The solid curves represent the upper and lower values recommended by Paterson and Budd (1982), and the dashed curve the best-fit relations (2.14) and (2.15) determined by Hooke (1981).

in this figure are the minimum and maximum values recommended by Paterson and Budd (1982). The uncertainty in the value of the rate factor implies that, for a given stress and temperature, the strain rate may vary by as much as a factor of 5. Hooke (1981) discusses possible explanations for why the different experiments yield such wide scatter. Factors that may play a role are melting effects in the ice samples, variations in grain size, impurity content, and ice density. However, perhaps most important is the effect that ice fabric has on the creep rate. Before discussing this issue, the next section delves into alternative (isotropic) flow laws that have been proposed for glacier modeling.

2.3 MORE ABOUT THE CONSTITUTIVE RELATION

Nye's generalization of Glen's law, discussed in the previous section, is commonly used to describe the rheological properties of glacier ice. However, the form of this relation has not been confirmed unambiguously. On the contrary, it can be argued that many laboratory experiments have disproven the applicability of Glen's law. As early as 1958, Glen recognized that the few experimental results available at that time disagreed with the simple flow law (2.10). Based on theoretical arguments, summarized below, Glen (1958) presented a more general constitutive relation.

Making the assumption that ice is isotropic implies that the strain-rate tensor must possess the same symmetry as the full stress tensor. This means that the strain-rate tensor must be a polynomial function of the stress tensor. That is

$$\dot{\varepsilon} = \sum_{k=0}^{K} F_k \, \sigma^k, \tag{2.16}$$

where the F_k represents arbitrary functions of the three invariants of the stress tensor. A particular strain-rate component is then given by

$$\dot{\varepsilon}_{ij} = F_1 \, \delta_{ij} + F_2 \, \sigma_{ij} + F_3 \, \sigma_{ik} \, \sigma_{kj} + F_4 \, \sigma_{ik} \, \sigma_{kl} \, \sigma_{lj} + \cdots\cdots. \tag{2.17}$$

The fourth and further terms on the right-hand side can be written in terms of the first three terms using the Hamilton–Cayley theorem (Truesdell and Noll, 1965, p. 26)

$$\sigma_{ij}^3 - I_1 \, \sigma_{ij}^2 - I_2 \, \sigma_{ij} - I_3 \, \delta_{ij} = 0, \tag{2.18}$$

where the I_i represent the three invariants of the full stress tensor, and $\delta_{ij} = 1$ if $i = j$ and $\delta_{ij} = 0$ if $i \neq j$ (the Kronecker delta).

To eliminate the effect of hydrostatic pressure on the rate of deformation, the strain rates are linked to deviatoric stresses, τ_{ij}, defined in Section 1.2. From the above it follows immediately that the most general constitutive relation is

$$\dot{\varepsilon}_{ij} = F_1 \, \delta_{ij} + F_2 \, \tau_{ij} + F_3 \, \tau_{ik} \, \tau_{kj}. \tag{2.19}$$

A further simplification is possible if the ice is taken to be incompressible; that is, the density of the ice remains constant during deformation. Because the change in density is directly related to the first invariant of the strain-rate tensor, incompressibility requires that (c.f. Section 1.2)

$$\dot{\varepsilon}_{xx} + \dot{\varepsilon}_{yy} + \dot{\varepsilon}_{zz} = 0. \tag{2.20}$$

Using equation (2.19) to determine the strain rates, and noting that the three normal deviatoric stresses sum to zero, gives the following relation:

$$F_1 = -\frac{2}{3} I_2 F_3. \tag{2.21}$$

The flow law can now be written in the general form

$$\dot{\varepsilon}_{ij} = F_2(I_2, I_3)\tau_{ij} + F_3(I_2, I_3)\left(\tau_{ik}\tau_{kj} - \frac{2}{3} I_2 \delta_{ij}\right), \tag{2.22}$$

where I_2 and I_3 are the second and third invariants of the deviatoric stress tensor, as defined in Section 1.1. Only if the second term on the right-hand side is neglected and also the dependency of the first term on the third invariant is ignored does this expression reduce to the commonly used constitutive relation.

By neglecting the second term on the right-hand side of equation (2.22), normal stress effects are tacitly excluded. However, Reiner (1945) predicted on theoretical grounds that normal stress effects (or dilatancy, a term coined by Reynolds in 1885) should be present in any viscous material whose rheological properties are described by a nonlinear functional relationship between deviatoric stress and strain rate. Most non-Newtonian fluids for which suitable measurements have been made exhibit non-zero and unequal normal stress differences in shearing flow (Schowalter, 1978). To illustrate the manifestation of normal stress effects, consider the situation in which only a shear stress, τ_{xz}, is applied. From the constitutive relation (2.22) the strain-rate tensor is found to be

$$\begin{pmatrix} \dot{\varepsilon}_{xx} & \dot{\varepsilon}_{xy} & \dot{\varepsilon}_{xz} \\ \dot{\varepsilon}_{xy} & \dot{\varepsilon}_{yy} & \dot{\varepsilon}_{yz} \\ \dot{\varepsilon}_{xz} & \dot{\varepsilon}_{yz} & \dot{\varepsilon}_{zz} \end{pmatrix} = F_2 \begin{pmatrix} 0 & 0 & \tau_{xz} \\ 0 & 0 & 0 \\ \tau_{xz} & 0 & 0 \end{pmatrix} + \frac{1}{3} F_3 \begin{pmatrix} \tau_{xz}^2 & 0 & 0 \\ 0 & -2\tau_{xz}^2 & 0 \\ 0 & 0 & \tau_{xz}^2 \end{pmatrix}. \tag{2.23}$$

Thus, there is a swelling or contraction perpendicular to the plane of shear, given by

$$\dot{\varepsilon}_{yy} = -\frac{2}{3} F_3 \tau_{xz}^2, \tag{2.24}$$

and a corresponding contraction or swelling in the other two directions (that is, in the plane of shear), such that the volume does not change. If the material is laterally constrained, for example by rigid walls, an extra pressure is exerted upon these walls.

Although Glen (1958) discussed these normal stress effects, this phenomena has received very little attention in glaciology. Two papers in which these effects are addressed are those of McTigue et al. (1985) and Man and Sun (1987). From these analyses it appears that the manifestation of normal stress effects on glaciers may be small. McTigue et al. (1985) calculate that these effects may cause a depression of several meters in the free surface of a glacier in an open channel. However, Man and Sun (1987) argue that this surface depression (or heave) is considerably smaller. Despite the apparent smallness of these effects, Van der Veen and Whillans (1990) find that inclusion of normal stress effects into the constitutive relation may be important in explaining the small-scale flow features observed near Dye-3, Greenland, but whether such a modified flow law has much impact on the large-scale dynamics of ice sheets remains to be demonstrated.

While Glen's law with exponent n = 3 is widely adopted for glacier modeling, many laboratory experiments indicate that this value may be smaller ($n \leq 2$) at low deviatoric stresses (< 100 kPa) common in glaciers. Earlier studies may be suspect because the slow deformation rates involved make it unclear whether steady-state creep was achieved (Weertman, 1973a). More recent experiments, however, have convincingly demonstrated the existence of a transitional stress value where the exponent changes as different physical processes become more or less dominant (for example, Durham et al., 2001; Goldsby and Kohlstedt, 2001; Goldsby, 2006). Three different creep regimes can be identified. At low stresses, deformation proceeds primarily by grain boundary sliding with n = 1.8 (termed *superplastic flow*), while at higher stresses dislocation creep becomes dominant and n = 4. Contrary to dislocation creep, grain boundary sliding is strongly dependent on grain size. At very low stresses and for the smallest grain sizes, basal slip accommodated by grain boundary sliding is most important, with n = 2.4 (Goldsby, 2006; Goldsby and Kohlstedt, 2001). A fourth mechanism was proposed by Goldsby and Kohlstedt (2001), namely, diffusional flow, but could not be observed at practical laboratory strain rates.

Based on experimental results, Goldsby and Kohlstedt (2001) propose the following constitutive relation

$$\dot{\varepsilon} = \dot{\varepsilon}_{\text{diff}} + \left(\frac{1}{\dot{\varepsilon}_{\text{basal}}} + \frac{1}{\dot{\varepsilon}_{\text{gbs}}} \right)^{-1} + \dot{\varepsilon}_{\text{disl}}, \tag{2.25}$$

where the subscripts refer to diffusional flow (diff), basal or easy slip (basal), grain boundary sliding (gbs), and dislocation creep (disl). Each strain rate on the right-hand side is described by a power law of the form

$$\dot{\varepsilon} = A \frac{\sigma^n}{d^p} \exp\left(-\frac{Q + PV}{RT} \right), \tag{2.26}$$

where A and n are flow parameters, σ is the differential stress, d is grain size with p the corresponding exponent, Q is the activation energy for creep, P is the hydrostatic pressure, V is the activation volume for creep, R is the gas constant, and T is absolute temperature. Values for the various parameters for each creep mechanism are given in Goldsby and Kohlstedt (2001).

Goldsby (2006) considers the flow at Byrd Station, West Antarctica, and compares grain size at depth measured in the deep ice core with shear stress at depth and concludes that the ice probably deforms by grain boundary slip over nearly the entire ice thickness. Only near the base of the ice sheet is the ice expected to deform in a transitional regime between creep limited by grain boundary slide and dislocation creep. This conclusion may be questioned because the only stress considered is the shear stress, τ_{xz}, assumed to increase linearly with depth (as in the lamellar flow model discussed in Section 4.2). However, other stress components, in particular the along-flow stretching stress, τ_{xx}, are believed to be important (Whillans and Johnsen, 1983), and hence Goldsby (2006) may have underestimated the differential stress. To adequately test the applicability of the flow law (2.25) would require a full-stress model and comparison with model predictions against observations, as was done by Van der Veen and Whillans (1990) for flow along the Dye-3, Greenland, strain network.

An interesting consequence of the Goldsby–Kohlstedt flow law is that this law seems to eliminate the need to account for crystal anisotropy. The role of fabric development on glacier deformation and flow is discussed more in the next two sections, but in short, ice near the base of ice sheets often exhibits a single-orientation fabric with the crystal c-axes oriented vertically upward. This anisotropy renders the ice relatively soft with respect to shear stresses, and to accommodate this effect, the rate factor in Glen's flow law is multiplied with an *enhancement factor* where crystal anisotropy is expected. For grain boundary sliding, the strain rate is proportional to $1/d^{1.4}$ where d represents grain size. In deeper and older ice, a reduction in grain size compared with that of younger ice is often observed, possibly associated with the Holocene—Last Glacial Maximum climatic transition (Weiss et al., 2002). Thus, creep rates associated with grain boundary sliding will increase in the lower ice layers, thereby eliminating the need for introducing an enhancement factor.

Peltier et al. (2000) adopt the Goldsby–Kohlstedt flow law (2.25) to model the shape of the Laurentide Ice Sheet during the Last Glacial Maximum using a coupled thermomechanical model tuned to the present-day Greenland Ice Sheet. Pettit and Waddington (2003) apply a similar two-term flow law to model ice flow around ice divides where deviatoric stresses are small. Peltier et al. (2000) claim that the model based on the flow law (2.25) gives a height-to-width ratio in better agreement with the inferred geometry during the Last Glacial Maximum than does the model based on Glen's flow law (2.10). The comparison is somewhat qualitative, and the new rheology essentially replaces one unknown parameter, the enhancement factor at depth to account for anisotropy in crystal fabric, with another unknown parameter, grain size. Without additional observations and more stringent comparison protocols, it remains unclear whether the Goldsby–Kohlstedt law represents an improvement over Glen's law when it comes to large-scale ice-sheet modeling.

Glen's flow law (and variations on it; c.f. Hutter, 1983) applies to isotropic ice. Where the ice has developed a strong anisotropy (for example, a vertical clustering of the crystal c-axes), none of these relations adequately describes the rheological properties. Therefore, the next two sections discuss how fabric affects the deformation of glacier ice.

2.4 FABRIC EFFECTS IN GLACIER ICE

The typical creep curve shown in Figure 2.3 may reflect changes in the fabric pattern of polycrystalline ice as it is being deformed. Azuma and Higashi (1985) found that compression of an initially random fabric results in a clustering of c-axes around the compressional axis; tension causes the c-axes to rotate away from the tensile axis (Fujita et al., 1987). Similar results have been found for metallic crystals (c.f. Nicolas and Poirier, 1976). Based on geometrical considerations, Boas and Schmid (1931) showed why such crystal rotation occurs.

Referring to Figure 2.5 for the case of crystals deforming by basal glide only, lateral constraints imposed by neighboring crystals allow only deformation as shown in the figure. That is, there is no rotation of lines perpendicular to the compressive axis or parallel to the tensile axis (the basis for this assumption is not entirely clear). Under these conditions, geometry shows that the c-axis rotates toward the compressional axis and away from the tensile axis. This fabric development has important consequences for the rate of deformation.

Consider as an example an aggregate of polycrystalline ice with a random fabric; that is, all orientations of crystal c-axes are equally probable. If the sample is subjected to uniaxial compression, deformation causes the c-axes of individual crystals to rotate toward the compressive axis. The rate of rotation is dependent on the strain of the crystal, so that crystals that are oriented optimally for basal glide (at an angle of 45° to the compressive axis) are rotated the most because these crystals have the largest shear stress acting on their basal planes. However, because the rotation causes the crystals to be oriented less favorably for deformation by basal glide, the resolved basal shear stress decreases and their rate of deformation decreases. Ultimately, when all crystals have rotated toward the compressive axis and the resolved shear stress on their basal planes is almost zero, very little deformation occurs.

Van der Veen and Whillans (1994) use a numerical model to simulate the development of fabric in an ice sample subjected to stress. Their model is based on the assumptions that crystals deform by basal glide only, and that the stress is uniform throughout the aggregate. Rotation of the crystal c-axes is calculated somewhat differently than shown in Figure 2.5, but this difference is not crucial to the results. They start their model simulations with 400 crystals whose c-axes are distributed randomly. Calculated creep curves are shown in Figure 2.6.

In the simulations in which recrystallization is not included (curves labeled "No Re-X"), the bulk strain rate decreases as the sample deforms, due to the progressive rotation of crystal c-axes toward orientations unfavorable for further deformation by basal glide. This rotation causes the aggregate to become harder so that the rate of deformation of the aggregate (which is simply the sum of all crystal deformations) decreases with increasing strain. Thus, primary creep (the stage of decreasing strain

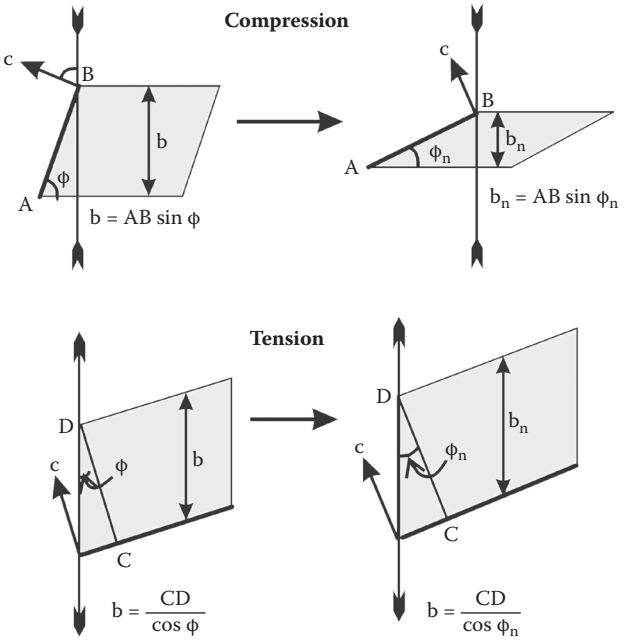

FIGURE 2.5 Geometrical basis for the Taylor–Bishop–Hill model, illustrating the rotation of a crystal c-axis. The heavy side of the crystal represents the basal plane, with the c-axis perpendicular to it. Under compression, the c-axis rotates toward the compressive axis and the new zenith angle and crystal strain are related as $\varepsilon = (b_n - b)/b = \sin\phi_n/\sin\phi - 1$. For deformation under tension, the crystal c-axis rotates away from the tensile axis, and $\varepsilon = (b_n - b)/b = \cos\phi_n/\cos\phi - 1$. (Reprinted from Van der Veen, C. J., and I. M. Whillans, *Cold Reg. Sci. Techn.*, 22, 171–195, 1994. With permission from Elsevier.)

rate; Figure 2.3) may be caused by crystal rotation rather than by the formation of dislocation tangles, or other microscopic processes suggested by Weertman (1973a) and Schulson and Duval (2009). It may be noted that after a few percent bulk strain, the c-axes distribution is almost the same as the initial random fabric. Nevertheless, the rotation of crystals since the start of deformation is sufficient to cause an appreciable decrease in strain rate.

If the sample is deformed for a sufficiently long time, the rate of deformation approaches zero. In Nature this does not happen because of recrystallization. This is an important softening process in which old, strained crystals are replaced by new and strain-free crystals. The experiments of Kamb (1972) suggest that the new crystals are formed at directions that are optimal for deformation by basal glide. In the case of uniaxial compression, this direction is at an angle of 45° to the compressive axis, and the recrystallization fabric is a girdle with a half-angle of 45° around this axis. Because the new crystals are oriented optimally for basal glide, the rate of deformation increases again after the onset of recrystallization.

Van der Veen and Whillans (1994) make the assumption that a crystal recrystallizes after it has accumulated a certain threshold strain. The resulting creep curves

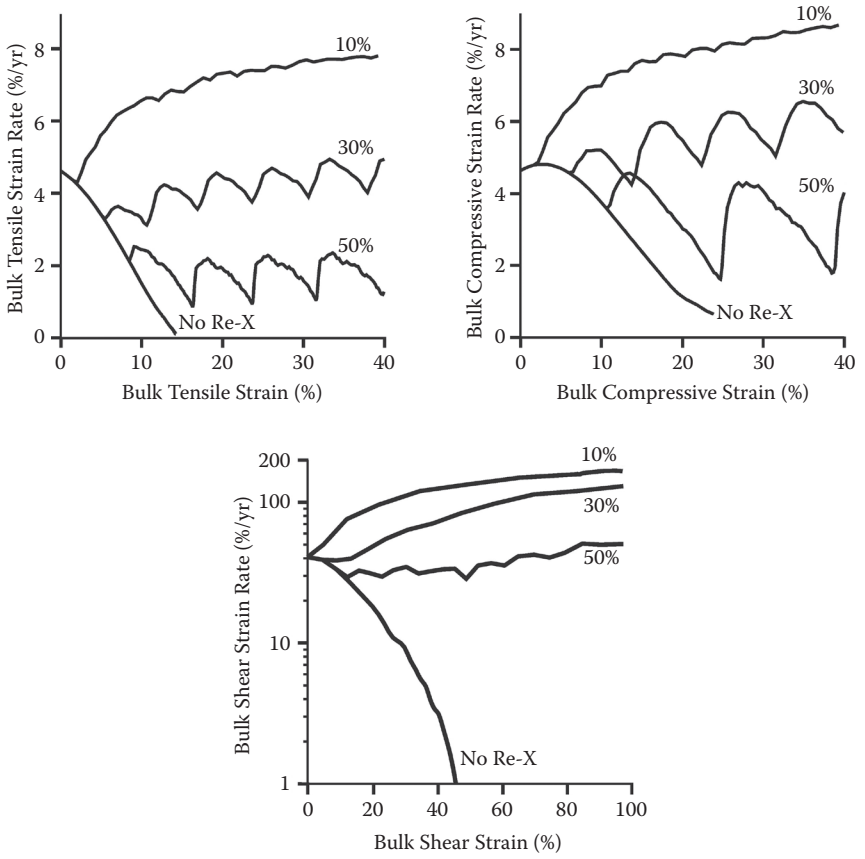

FIGURE 2.6 Modeled change in bulk strain for an aggregate of 400 crystals for uniaxial extension, uniaxial compression, and simple shear. The labels indicate the value of the threshold strain for recrystallization used in each simulation. The curves labeled "No Re-X" correspond to the simulations that do not include recrystalization and clearly show how the rate of deformation decreases with continued deformation, reaching almost zero after all crystals have rotated toward the "stiff" orientations. Note that the strain-rate scale for simple shear is logarithmic. (Reprinted from Van der Veen, C. J., and I. M. Whillans, *Cold Reg. Sci. Techn*., 22, 171–195, 1994. With permission from Elsevier.)

(Figure 2.6) are strikingly similar to those measured in laboratory experiments. The stage of decreasing strain rate (primary creep) is followed by tertiary creep, in which recrystallization makes the ice softer and the bulk strain rate increases and continues to do so until all crystals are aligned optimally. The increase in strain rate may be approximately continuous if the value for the threshold strain for recrystallization is small, or the increase in bulk strain rate may occur in discrete steps (for larger values of the threshold strain), as suggested by Hooke and Hudleston (1980). In the latter case, periods of recrystallization alternate with periods of crystal rotation and strain hardening. Unfortunately, no laboratory experiments have been carried out to

sufficiently large strains to determine whether such quasi-cyclic behavior exists or not.

The creep curves shown in Figure 2.6 support the suggestion by Budd and Jacka (1989) that the concept of steady-state secondary creep is misleading. The curves suggest that only two creep stages exist, namely, primary creep (decreasing bulk strain rate) and tertiary creep (increasing strain rate). The minimum creep rate reached during the deformation ("secondary creep") simply marks the onset of recrystallization.

There thus exists an important feedback between ice deformation and fabric development. Recrystallization causes the aggregate to become softer with respect to the applied stress, and continued deformation makes the ice much softer than ice with randomly oriented crystals. This may be the case for the basal ice in Greenland, characterized by vertical clustering of the directions of crystallographic c-axes. The dominant stress at depth is the vertical shear stress, and crystals are oriented optimally for deformation by basal glide. As a result, the shear strain rates are about three times as large as those that would occur if the ice had a random fabric (Dahl-Jensen, 1985). In the common terminology, the enhancement factor is about 3 for this ice.

Van der Veen and Whillans (1994) calculate a maximum softening factor of 2.5 for ice under uniaxial compression, and 4.3 for ice subjected to simple shear (using a nonlinear single-crystal flow law). These values are referenced to the initial strain rate. Common practice in laboratory experiments is to use the minimum strain rate as reference. Russell-Head and Budd (1979) argue that at such low strains, significant recrystallization has not yet occurred and the sample crystallography can be considered that of the initial sample. However, during the initial phase of deformation, rotation of crystals causes the ice to become gradually stiffer with respect to the applied stress. The minimum strain rate just before the onset of recrystallization does not correspond to the rate of deformation of a randomly oriented aggregate. Depending on the threshold strain for recrystallization, the difference between initial and minimum strain rate may be as much as a factor of 1.5 (Figure 2.6). Because the value of the minimum strain rate depends on the unknown value of the threshold strain, Van der Veen and Whillans (1994) chose the initial strain rate as reference. Consequently, their enhancement factors may be expected to be smaller than those given in the literature.

The softening effect of developing fabric is larger for deformation under simple shear than for uniaxial compression. This is in agreement with other studies summarized in Budd and Jacka (1989). These studies indicate that for uniaxial deformation, the total softening from the minimum strain rate to the steady-state value is about 3, while for simple shear the enhancement factor is about 8.

2.5 CREEP IN AXIALLY SYMMETRIC ICE

Continued deformation and recrystallization leads to special fabric patterns in which the crystal c-axes are clustered around a limited number of orientations. Such a fabric makes the ice anisotropic; that is, the ice may be softer with respect to certain stresses and harder with respect to others than ice with randomly oriented crystal c-axes. A common example is the single-maximum fabric that develops in

ice subjected to simple shear, characterized by all crystal c-axes oriented in the direction of the vertical axis. Such ice is said to be axially symmetric, or transversely isotropic. This means that with the axis of symmetry in the z-direction, say, the ice has a different stiffness with respect to the shear stresses τ_{xz} and τ_{yz} than with respect to stresses in the other directions (τ_{xx}, τ_{yy}, or τ_{xy}). The stiffness is the same for both normal stresses, τ_{xx} and τ_{yy}.

The softening of ice with a single maximum fabric is commonly described by an enhancement factor. That is, the rate factor, A, in the constitutive relation (2.10) is multiplied by a depth-dependent enhancement factor, whose value is larger than 1. This is an expedient technique, but strictly speaking, it does not account for anisotropy of the ice. The softening of the ice must be described by a tensor. For example, an aggregate in which all c-axes are aligned vertically may be expected to be stiffer with respect to longitudinal stresses, and softer with respect to shear stresses, than isotropic ice with a random fabric. This effect cannot be described by a single enhancement factor.

A number of anisotropic constitutive relations for polar ice have been suggested. Most of these are based on results from laboratory experiments and are not yet fully supported by a mathematical theory (for example, Lile, 1978; Baker, 1981, 1982; Jacka and Budd, 1989). A theoretically more sound constitutive relation was formulated by Johnson (1977). In somewhat modified form, this relation was applied to glacier ice by Lliboutry and Andermann (1982), Pimienta and others (1987), and Van der Veen and Whillans (1990). The derivation of the last authors (based on Johnson, 1977) is summarized below.

Van der Veen and Whillans (1990) show that the isotropic constitutive relation (2.10) can also be written as

$$\dot{\varepsilon}_{ij} = \frac{\partial W}{\partial \sigma_{ij}}, \tag{2.27}$$

with

$$W = \frac{2}{n+2} A \, \tau_e^{n+1}, \tag{2.28}$$

the dissipation potential. Because the effective stress, τ_e, is a function of the second invariant of the deviatoric stress tensor (equations (2.3) and (2.7)), the generalized flow law is based on the assumption that the dissipation potential is a function of the second invariant only.

Ericksen and Rivlin (1954) discuss the requirements for the dissipation potential that applies to the case of axially symmetric ice with the axis of symmetry in the z-direction. Noting that the first invariant of the stress deviator is zero by definition, and neglecting any effects of the third invariant (as in the isotropic case), these authors show that W can only be a function of the following three quantities

$$\tau_{xx}^2 + \tau_{yy}^2 + \tau_{zz}^2 + 2\tau_{xz}^2 + 2\tau_{yz}^2 + 2\tau_{xy}^2, \tag{2.29}$$

$$\tau_{zz}, \tag{2.30}$$

and

$$\tau_{xz}^2 + \tau_{yz}^2 + \tau_{zz}^2. \tag{2.31}$$

Based on this result, Van der Veen and Whillans (1990) introduce the following three invariants

$$T_1^2 = \tau_{zz}^2, \tag{2.32}$$

$$T_2^2 = \tau_{xx}^2 + \tau_{yy}^2 + 2\tau_{xy}^2, \tag{2.33}$$

and

$$T_3^2 = \tau_{xz}^2 + \tau_{yz}^2. \tag{2.34}$$

Any combination of these three quantities can be used to construct the dissipation potential. The simplest form that is reducible to expression (2.28) for the isotropic case, is

$$W = \frac{1}{m} A G^m, \tag{2.35}$$

with

$$\begin{aligned} G &= \frac{\alpha}{2} T_1^2 + \frac{\beta}{2} T_2^2 + \frac{\gamma}{2} T_3^2 = \\ &= \frac{1}{2}\left(\alpha\tau_{zz}^2 + \beta\tau_{xx}^2 + \beta\tau_{yy}^2\right) + \beta\tau_{xy}^2 + \frac{\gamma}{2}\left(\tau_{xz}^2 + \tau_{yz}^2\right). \end{aligned} \tag{2.36}$$

After some tedious tensor arithmetic, the following expressions for the strain-rate components can be derived:

$$\dot{\varepsilon}_{xx} = A G^{m-1}\left(\beta\tau_{xx} + \frac{1}{3}(\beta-\alpha)\tau_{zz}\right), \tag{2.37}$$

$$\dot{\varepsilon}_{yy} = A G^{m-1}\left(\beta\tau_{yy} + \frac{1}{3}(\beta-\alpha)\tau_{zz}\right), \tag{2.38}$$

$$\dot{\varepsilon}_{zz} = A G^{m-1}\left(\frac{2}{3}\alpha + \frac{1}{3}\beta\right)\tau_{zz}, \tag{2.39}$$

$$\dot{\varepsilon}_{xz} = A G^{m-1}\left(\frac{\gamma}{2}\tau_{xz}\right), \tag{2.40}$$

$$\dot{\varepsilon}_{yz} = A G^{m-1}\left(\frac{\gamma}{2}\tau_{yz}\right), \tag{2.41}$$

$$\dot{\varepsilon}_{xy} = A G^{m-1}(\beta\tau_{xy}). \tag{2.42}$$

Comparison of these expressions with the isotropic flow law (2.11) shows that the anisotropic constitutive relation reduces to Glen's law for $\alpha = \beta = 1$ and $\gamma = 2$, and the exponent $m = (n + 1)/2$.

It should be noted that the anisotropic constitutive relation proposed by Van der Veen and Whillans (1990) is only applicable to glacier ice in which the c-axes are clustered around the vertical direction. A more general theory should also include an equation describing the change with time of the axis of symmetry (i.e., the c-axes direction). More general theories have been developed by Green (1964a,b) and in a series of papers by Ericksen (Truesdell and Noll, 1965, p. 523, discuss Ericksen's theory and provide the references to the original papers). Few attempts have been made as of yet to apply these theories to glacier ice. Because vertical clustering of c-axes has been observed at many sites where the flow is dominated by vertical shear, it seems appropriate to first investigate theories for anisotropy that can explain observed patterns of flow with a given configuration of c-axes. If such theories fail to explain the observations, there is little point in taking the next step and developing complex theories that also include explicit calculation of the time-evolution of the orientation of the axis of symmetry.